



## A Search for $WH$ Production at $\sqrt{s} = 1.96$ TeV

The DØ Collaboration

URL: <http://www-d0.fnal.gov>

(Dated: March 19, 2006)

A search for  $WH$  production in  $p\bar{p}$  collisions at a center of mass energy of  $\sqrt{s} = 1.96$  TeV is presented. Events containing one lepton, missing transverse energy, and one or two  $b$ -tagged jets are considered. The analysis is performed separately in the  $e$  and  $\mu$  channel, with a further subdivision between events having one and two  $b$  tagged jets in the final state. The integrated luminosity used in these analyses has been accumulated by the DØ experiment at the Tevatron collider and averages to  $378 \text{ pb}^{-1}$ . In the single and double  $b$ -tagged samples, good agreement between data and the standard model is observed. The combined result for both leptons and in both final states provides upper limit on  $WH$  production cross section ranging from 2.4 pb to 2.9 pb for Higgs masses between 105 and 145 GeV.

*Preliminary Results for Winter 2006 Conferences*

For Higgs searches, the most sensitive production channel at the Tevatron for a Higgs mass below  $\sim 140$  GeV is the associated production of a Higgs boson with a  $W$  boson. A search for  $WH$  production in the  $e\nu b\bar{b}$  decay channel using  $174 \text{ pb}^{-1}$  of  $D\bar{O}$  data has already been published [1]. An update of that result using the same dataset as considered in this analysis was released in 2005 [2]. The  $\mu\nu b\bar{b}$  decay channel however had not yet been analysed. Its study is reported here and combined with the electron channel, which has also been reoptimized. The data set corresponds to an integrated luminosity of  $371 \text{ pb}^{-1}$  ( $e$ -channel) and  $385 \text{ pb}^{-1}$  ( $\mu$ -channel). One lepton (electron or muon), missing transverse energy  $\cancel{E}_T$  to account for the neutrino in the  $W$  boson decay and exactly two jets are required, with at least one of the jets being  $b$ -tagged. In double  $b$ -tagged events, the dominant backgrounds to  $WH$  are  $Wb\bar{b}$  production,  $t\bar{t}$ , and single top quark production. In single  $b$ -tagged events, multijet events and  $W$  production in association with  $c$  and/or light jets also provide important contributions to the background. It has been shown [1] that the signal to background ratio can be improved by requiring exactly two jets, so we concentrate on this signature in this analysis.

## II. DATA SAMPLE AND EVENT SELECTION

The analysis relies on the following components of the  $D\bar{O}$  detector: a central-tracking system, which consists of a silicon microstrip tracker (SMT) and a central fiber tracker (CFT), both located within a 2 T superconducting solenoidal magnet [3]; a liquid-argon/uranium calorimeter made of a central section (CC) covering  $|\eta|$  up to  $\approx 1.1$ , and two end calorimeters (EC) extending coverage to  $|\eta| < 3.2$ , all housed in separate cryostats [4], with scintillators between the CC and EC cryostats providing sampling of developing showers at  $1.1 < |\eta| < 1.4$ ; a muon system which resides beyond the calorimetry, and consists of a layer of tracking detectors and scintillation trigger counters before 1.8 T toroids, followed by two more similar layers after the toroids; the tracking at  $|\eta| < 1$  relies on 10 cm wide drift tubes [4], while 1 cm mini-drift tubes are used at  $1 < |\eta| < 2$ .

The luminosity is measured using plastic scintillator arrays located in front of the EC cryostats, covering  $2.7 < |\eta| < 4.4$ . The trigger and data acquisition systems are designed to accommodate the large luminosity of Run II. We reject data periods in which the quality of the data of the tracking (CFT and SMT), the calorimeter or the muon system may be compromised. The uncertainty on the measured luminosity is 6.5% [5].

The  $W$  + jets candidate events must pass one of the triggers requiring for the  $e$  channel at least one electromagnetic (EM) object and for the  $\mu$  channel, at least one muon object or a “muon + jet” trigger. The calorimeter data are zero-suppressed (at  $2.5 \sigma$ , where  $\sigma \equiv$  RMS of the cell noise), and in the event reconstruction we use the T42 calorimeter reconstruction algorithm [6], which suppresses all cells with negative energy and single isolated cells between  $2.5 \sigma$  and  $4 \sigma$  before the other calorimetric algorithms are applied. This has been shown to improve the calorimeter performance [7].

### A. Selection and Lepton identification

The event selection for this analysis requires one lepton with  $p_T > 20$  GeV, missing transverse momentum  $\cancel{E}_T > 25$  GeV and two jets with  $p_T > 20$  GeV and pseudorapidity  $|\eta| < 2.5$ . Only events having a  $z$  vertex within  $\pm 60$  cm of the nominal interaction point are kept. If the lepton is an electron, it is required to be in the central region, i.e. to have  $|\eta_{detector}^e| < 1.1$ . If it is a muon the requirement is  $|\eta_{detector}^\mu| < 2.0$ .

The electrons are identified in 2 steps: a) the preselected electron candidates are first required to pass stricter identification (ID) criteria: EM fraction  $> 0.9$ , isolation  $< 0.10$ , stricter shower shape requirements; these criteria define a “loose” electron. b) The loose electrons are then tested with a likelihood algorithm developed on well controlled samples, and which takes as input 7 quantities sensitive to the EM nature of the particles. If they satisfy the likelihood requirement, they become final (“tight”) electrons for the analysis. The efficiency of the ID and likelihood requirements are determined from a dielectron sample in which we select a pure set of  $Z$  events. The ID/reconstruction efficiency is found to be  $95.4 \pm 0.4\%$ . The likelihood efficiency for electrons is determined to be  $92\% \pm 0.3\%$ .

Muons are reconstructed using information from the muon detector and the central tracker. They are required to have hits in all layers of the muon system inside and outside the toroid steel. The superior spatial resolution of the central tracker is used to improve the accuracy of kinematic properties of the muon and to confirm that the muon originated from the primary vertex. A veto against cosmic based on scintillator hits timing is applied. Quality criteria on the associated central track are also applied to reject the majority of fake muons. A small ( $< 3\sigma_{dca}$ ) track impact parameter ( $dca$ ) significance is required to reject muons originating from semi-leptonic decays of heavy flavored hadrons which constitutes the main background. Such background muons have a lower transverse momentum spectrum and

are typically non-isolated due to jet fragmentation of the partial hadronic decay. A loose isolation criterion is defined by the spatial separation  $\Delta R$  between a muon and a jet in the  $\eta$ - $\varphi$  plane, where  $\varphi$  is the azimuthal angle: we require the distance between a muon and the closest jet to be  $\Delta R(\mu, \text{jet}) > 0.5$ . Tighter muon isolation criteria are defined by requiring that: a) the scalar sum of the transverse energy of calorimeter clusters in a hollow cone around the muon between  $\Delta R = 0.1$  and  $\Delta R = 0.4$  is less than 2.5 GeV, and b) the scalar sum of the transverse momentum of all tracks within a cone of radius  $\Delta R = 0.5$  around the muon is less than 2.5 GeV. The track matched to the muon is excluded from this sum.

## B. Multijet (QCD) background

To estimate the number of multijet (QCD) events containing a jet passing the final lepton identification criteria we determine from the data the probability  $p_{tight}^{loose}$  for a “loose” lepton originating from a jet to pass the tight lepton cut. This is done separately for the electron and the muon channel. We use a sample of events having 2 jets back to back in  $\varphi$  ( $|\pi - \Delta\varphi| < 0.2$ ), at low  $\cancel{E}_T (< 10 \text{ GeV})$ , in which one of the jets has an EM fraction smaller than 0.7 and is required to be in the central calorimeter and far from the modules boundaries. In the electron case, the other jet is required to satisfy all the electron-ID requirements except the likelihood cut. The probability  $p_{tight}^{loose}$  is obtained by dividing the number of events containing at least one electron candidate passing the likelihood cut by the total number of events of the sample. This probability is determined as a function of the  $p_T$  of the candidate electron. The QCD background is then estimated for every differential distribution: we use this  $p_T$  dependent probability in the so-called matrix method [8] that we apply to our final sample and to the loose sample (defined as the sample in which all the event selection criteria are applied but for the electron likelihood). In the muon case, the same procedure is applied using the corresponding tight and loose requirements.

The  $p_T$  distribution of the lepton in the final  $W + 2$  jet sample is shown in Fig. 1a, and compared to the expectation: at low  $p_T$  the contamination of QCD background as determined by the matrix method is visible. The shape and magnitude of the distribution is well reproduced by the simulation of the  $W + \text{jets}$  processes, after adding the QCD background and other standard model (SM) backgrounds detailed in the next section.

## C. Missing Transverse Energy and Jet properties

Since we want to select  $W$  decays we require large transverse missing energy:

$$\cancel{E}_T > 25 \text{ GeV}$$

$\cancel{E}_T$  is calculated from the calorimeter cells except for unclustered cells in the outermost layer (Coarse Hadronic) of the calorimeter, and is corrected for the presence of any muons. All energy corrections to electrons or to jets are propagated into  $\cancel{E}_T$ . The  $\cancel{E}_T$  distribution, shown in Fig. 1b, is well reproduced by the simulation when taking into account the QCD background which accumulates at low  $\cancel{E}_T$ .

The transverse mass of the  $W$  candidates in the  $W + \text{jets}$  sample is reconstructed from the lepton and missing transverse energy. Its distribution is shown in Fig. 1c. A good agreement in shape and amplitude is observed between the data and the simulation. In Fig. 1d the distribution of the scalar transverse energy is shown.

The jets used in this analysis are standard Run II cone jets with a radius of  $R = 0.5$  with standard  $D\phi$  jet-ID criteria to avoid fake jets which might originate from noise in the calorimeter. The following cuts ensure that the jet energy distribution in the various layers of the calorimeter is reasonable and that the jets are not due to spurious energy deposits: a) Energy fraction in the EM layers of a jet is required to be  $0.05 < EMF < 0.95$ . b) Energy fraction in the CH calorimeter is required to be  $CHF < 0.4$ . The effect of noise jets is strongly diminished by the use of the T42 algorithm which removes on average 15 GeV of noise per event [7].

The difference in efficiency of the jet-ID cuts between data and simulation is quantified in the overall jet reconstruction efficiency scale factor to which a systematic error of 5% (per jet) is assigned. The jet reconstruction efficiency has a little effect on the  $WH$  signal since the average  $p_T$  of the leading and second jet originating from a 115 GeV Higgs after the selection cuts, are approximately 80 and 40 GeV respectively. The  $p_T$  distributions of the leading jet and next to leading jet in  $W + 2$  jet events are shown in Figs. 2a and b. The  $\eta$  distribution of the leading jets is shown in Fig. 2c. These distributions are described by the simulation.

The distribution of the invariant mass of the two leading jets for the events in this sample is shown in Figs. 2 d) and compared to the simulation. We observe a good agreement in amplitude and shape for masses above 60 GeV.

The following processes have been simulated with the PYTHIA [9] MC event generator version 6.202, making use of the CTEQ5L [10] leading-order parton distribution functions:

- inclusive production of:  $W \rightarrow e/\mu/\tau + \nu$ ;  $Z \rightarrow ee/\mu\mu/\tau\tau$ ,  $WW$ ,  $WZ$ ,  $ZZ$ .
- $t\bar{t} \rightarrow e/\mu/\tau + \text{jets}$  production (lepton+jets and dilepton channels)
- $WH \rightarrow e/\mu/\tau + \nu + b\bar{b}$  production

The following processes are simulated using other generators:

- The single top ( $s$ -channel ( $tb$ ) and  $tbq$ -channel) are generated using COMPHEP [11].
- The  $W + \geq 2$  jets events (“ $W + \text{jets}$ ”), are generated with ALPGEN [12] (with PYTHIA radiation + hadronization) since ALPGEN has a better simulation of processes with large jet multiplicities. The generation is based on  $Wjj$  processes, including  $Wc\bar{c}$  and  $Wcj$ , but not  $Wb\bar{b}$  which is generated separately.
- The  $Wb\bar{b}$  events are generated with ALPGEN requiring 2 parton jets with  $p_T > 8$  GeV separated in  $\eta$ - $\varphi$  by  $\Delta R(\equiv \sqrt{\Delta\eta^2 + \Delta\varphi^2}) > 0.4$ . The NLO cross section is obtained using MCFM[13].

These simulated backgrounds are absolutely normalized, i.e. according to cross section, with the exception of the  $W + \text{jets}$  sample which is normalized to the data after subtraction of all the other backgrounds. The systematic uncertainty on the NLO cross sections of these processes is 6–18%, depending on the process.

All the above events were processed through the DØ detector simulation (DØgstar [14], based on GEANT), the electronics simulation (DØsim) and the reconstruction software (DØreco). The simulated events are then weighted by the trigger efficiency and by the ratio data/simulation of all the selection efficiencies.

#### IV. $b$ -TAGGING

The primary goal of this analysis is the search for  $WH$  production with two  $b$  jets in the final state. For tagging heavy flavored jets the  $b$ -tagging algorithm JLIP[15] has been used. It is based on the estimation of the probability to observe the  $b$  lifetime. The jet lifetime probability is constructed using only the tracks associated to the jets which have a positive impact parameter in the transverse plane. The sign of the impact parameter is defined positive when the scalar product  $\vec{d}_{perigee} \cdot \vec{p}_T(jet)$  is positive.  $\vec{d}_{perigee}$  is defined in the transverse plane by the primary vertex and the impact point.

First the jet lifetime probability cut is set to 1%. If two jets are tagged the event is selected as double  $b$ -tagged. Otherwise the cut is tightened to 0.1% and if one jet can be tagged the event is selected as single  $b$ -tagged. The values of these cuts have been optimized by maximizing the sensitivity to the Higgs signal. In this way the single and double  $b$ -tagged subsamples are independent, which simplifies their combination. The JLIP cuts correspond approximately to a mistag rate (tagging of light flavor jets) of the same amount, i.e. 0.1% and 1%. The efficiencies are  $33 \pm 4\%$  and  $55 \pm 4\%$  respectively. The efficiency has been determined with central “taggable” jets ( $|\eta| < 1.2$ ) having a transverse momentum of  $35 < p_T < 55$  GeV. A jet is “taggable” if at least 2 tracks (one with  $p_T > 1$  GeV, the other with  $p_T > 0.5$  GeV) are inside the  $\Delta R < 0.5$  cone defining the jet. The jet taggability is typically 80% in a two jet QCD sample with an uncertainty of 3% per jet.

In this analysis, for each tagged jet in the simulation, we apply the ratio between the expected taggability  $\times$  tagging efficiency in data versus simulation to reweight the simulated events. For the tagging efficiency of simulated  $b$  or  $c$  jets, we use  $p_T - \eta$  dependent data versus Monte-Carlo scale factors, determined from real  $b$  jets by the DØ  $b$ -ID group [16]. These are also applied to light quark jets, but rescaled to match in our simulated “ $W + \text{light jets}$ ” sample the yield of mistagged events expected using light jet tag rate functions which are determined independently using dedicated data samples [16].

#### V. SINGLE $b$ -TAGGED EVENTS

A  $\Delta R$  cut between the two leading jets is applied ( $\Delta R > 0.75$ ) in order to reduce the influence of  $b$ -jets induced by gluon splitting and to allow an unambiguous assignment in the simulation of the jet flavor. The simulated jet

flavor is defined as the “highest” flavor found in an  $\eta - \varphi$  cone with 0.3 radius, centered around the direction of the reconstructed jet, the flavors being ranked from lowest to highest as  $u, d, s, c, b$ .

We observe 112  $W + 2$  jet events having one and only one  $b$ -tagged jet (0.1% JLIP cut), and 25 events having both jets  $b$ -tagged (1% JLIP cut). We first concentrate on the events having only one  $b$ -tagged jet and will discuss the double  $b$ -tagged events in the next section.

The QCD background is estimated with the matrix method, using as the loose sample the  $W + 2$  jet sample in which the lepton is selected using the loose criteria. It amounts to  $18.0 \pm 6.3$  events.

In Fig. 3a the distribution of the invariant dijet mass is shown for the  $W + 2$  jet events having one jet  $b$ -tagged. The data are compared to the sum of the simulated standard model processes added to the multijet background. The observed agreement indicates that the simulation, which includes the different Standard Model processes, describes the data well. The different components are detailed in Table I.

A “single  $b$ -tagged” (ST)  $WH$  production limit can be extracted from this distribution after selecting the same mass windows as described in the next section for the “double  $b$ -tagged” (DT) selection. The number of observed/expected events in these mass windows are detailed in Table II.

## VI. DOUBLE $b$ -TAGGED EVENTS

When requiring only one  $b$ -tagged jet, the background due to  $W + 2$  light quark jets, top, and QCD processes is still over a factor four larger than the processes which have not yet been observed and which can be studied with the upgraded Tevatron:  $Wb\bar{b}$ , single top and Higgs production. To improve the signal versus background ratio, we study in this section the events in which the second jet is  $b$ -tagged.

Fig. 3c shows the  $p_T$  distribution of the  $b$ -tagged jets from  $W + 2$   $b$ -tagged jet events, compared to the simulated expectation. There are 50 data entries, corresponding to 25 events with two  $b$ -tagged jets. We expect that jets originating from  $Wb\bar{b}$  have on average a smaller  $p_T$  than those originating from  $t\bar{t}$  decays. The  $H_T$  [17] distribution of these events is shown Fig. 3b. The distribution of  $\Delta R$  obtained from the two  $b$ -tagged jets is shown in Fig. 3d. In Fig. 4a and c are shown the distribution of the  $W$  transverse mass and the dijet mass formed from the 2  $b$ -tagged jets (in b and d are shown the same plots in logarithmic scale). Both plots display good agreement and the  $W$  mass peak is now appearing in the double-tagged sample, with the higher statistics.

The 25 events observed are to be compared to an expected Standard Model background of  $27.9 \pm 4.2$  events. The expected QCD background as obtained from the matrix method is  $1.36 \pm 0.60$  events, starting from the corresponding tagged loose sample. For the other backgrounds we expect  $26.5 \pm 4.1$  events, and their origin is detailed in Table I. All these results and distributions show that the simulation describes the data. To estimate our present sensitivity, after reviewing the systematic uncertainties, we will derive a cross section limit for  $WH$  production.

	$W + 2$ jet	$W + 2$ jets (1 $b$ -tagged jet)	$W + 2$ jet (2 $b$ -tagged jets)
$WH$	$1.68 \pm 0.17$	$0.35 \pm 0.39$	$0.31 \pm 0.06$
$WW, WZ, ZZ$	$117.8 \pm 7.2$	$4.12 \pm 0.71$	$1.62 \pm 0.26$
$Wb\bar{b}$	$87.0 \pm 16.6$	$16.7 \pm 3.5$	$10.83 \pm 2.38$
$t\bar{t}$	$53.7 \pm 6.0$	$12.7 \pm 1.9$	$7.38 \pm 1.57$
Single top	$32.7 \pm 6.7$	$7.8 \pm 4.1$	$2.90 \pm 0.34$
QCD Multijet	$850 \pm 231$	$18.0 \pm 6.3$	$1.36 \pm 0.60$
$W$ + or $Z$ + jets	$6245 \pm 751$	$52.9 \pm 9.4$	$3.52 \pm 0.74$
Total expectation	$7388 \pm 817$	$111.8 \pm 17.0$	$27.9 \pm 4.2$
Observed Events	7388	112	25

TABLE I: Summary table for the  $\ell$  ( $e$  and  $\mu$ ) + 2 jets +  $\cancel{E}_T$  final state. Observed events in data are compared to the expected number of  $W + 2$  jet events before and after  $b$ -tagging in the simulated samples of  $WH$ , dibosons,  $Wb\bar{b}$  production, top production ( $t\bar{t}$  and single top), QCD multijet background, and “ $W$  or  $Z$  + jet” production.

## VII. SYSTEMATIC UNCERTAINTIES

The experimental systematic errors on the efficiencies or those due to the propagation of other systematic errors (trigger, energy calibration, smearing), which affect the signal and standard model backgrounds (QCD background excepted, because it is derived from data) are the following (ranges indicate different values for the  $e$  and  $\mu$  channel)

- 2–3% error from the trigger efficiency derived from the data sample used in this analysis.
- 3–4% error for the lepton identification and reconstruction efficiency.
- 3–4% for the lepton energy smearing and scale.
- 5% for the jet-id and jet reconstruction efficiency, per jet.
- 5% for the modelling uncertainty of the jet multiplicity in the simulation.
- 5% (12%) for  $WH$  ( $Wb\bar{b}$ ), due to the jet energy scale error.
- 3% for the jet taggability.
- 5–6% for the JLIP  $b$ -tagging efficiency, per jet. For the light quark jets these errors are 9% (in the DT case) and 13% (in the ST case).

Overall, for  $WH$  production, the experimental systematic error is 16–19%. The luminosity error is treated separately and amounts to 6.5%.

### VIII. $WH$ CROSS SECTION LIMIT

The expected contribution from the  $b\bar{b}$  decay of a standard model Higgs boson of 115 GeV, produced in association with a  $W$  boson and passing through the whole analysis chain, is shown in Fig. 4d and amounts to 0.31 events. The expected distribution fit to a Gaussian in the optimal mass window  $\pm 25$  GeV (as determined from simulation) has a relative resolution of 14%. Similar resolutions are obtained for the other mass points. The mean values are systematically shifted towards lower values, since no  $b$ -jet energy scale correction is applied. However this is not an issue, since the effect is similar in data and simulation as observed in  $Z \rightarrow b\bar{b}$  [18].

Higgs mass	105 GeV	115 GeV	125 GeV	135 GeV	145 GeV
$WH$	0.4	0.27	0.17	0.09	0.04
$WW, WZ, ZZ$	3.3	2.5	1.1	0.4	0.15
$Wb\bar{b}$	6.6	6.6	4.5	3.4	2.5
$t\bar{t}$	3.9	4.3	4.4	4.5	4.5
Single top	2.3	2.3	2.4	2.4	2.2
QCD / $W$ or $Z$ +jets	19.2	30.6	23.3	19.0	16.4
Total expectation	50.9	45.1	35.7	29.7	25.7
Data	40	32	32	27	27
$WH$	0.37	0.28	0.17	0.09	0.04
$WZ$	1.4	1.0	0.60	0.22	0.05
$Wb\bar{b}$	4.2	3.6	3.0	2.4	2.0
$t\bar{t}$	2.0	2.1	2.4	2.2	2.3
Single top	0.89	0.89	0.92	0.89	2.0
QCD / $W$ or $Z$ +jets	1.8	1.6	1.4	1.2	1.0
Total expectation	10.5	9.3	8.1	6.9	6.3
Data	7	6	7	6	6
Combined Cross section limit (pb)	2.4	2.4	2.9	2.8	2.6
Expected Cross section limit (pb)	4.0	3.5	3.4	3.0	2.8

TABLE II: Number of observed and expected events, in different mass windows for single (ST, top table) and double  $b$ -tagged events (DT, bottom table). The upper 95% C.L. cross section limits are given.

Six double  $b$ -tagged events (32 single  $b$ -tagged events) are observed in the dijet mass window of a 115 GeV Higgs. The expected standard model background for the double  $b$ -tagged events (including here  $Wb\bar{b}$ ) is  $9.3 \pm 1.8$  events and the expected  $WH$  signal is  $0.28 \pm 0.06$  event.

As in the ST we can derive limits for the  $e$  and  $\mu$  channel. The four individual analyses ( $e$ ,  $\mu$ , ST, DT) are then combined and limits are derived from the invariant dijet mass distribution, using a modified frequentist approach, the  $CL_S$  method [19, 20]. In this case, the binned distributions are summed over the log-likelihood ratio test statistic. Systematic uncertainties are incorporated into the signal and background expectations using Gaussian sampling of individual uncertainties. Correlations between uncertainties are handled by varying simultaneously for all channels

the fluctuations of identical sources. Limits are determined by scaling the signal expectations until the probability for the background-only hypothesis falls below 5% (95% CL).

This translates into a cross section limit for  $\sigma(p\bar{p} \rightarrow WH) \times B(H \rightarrow b\bar{b})$  of 2.4 pb at 95% C.L. limit for a Higgs boson mass of 115 GeV. The corresponding expected upper limit is 3.5 pb. The same study is performed for four other Higgs mass points which are 105, 125, 135, and 145 GeV. The corresponding observed events, expectations, and limits are given in Table II and summarized in the Higgs cross section limit plot, Fig. 5. Our result is compared to the previously published results of DØ on 174 pb<sup>-1</sup> of data in the  $e$  channel only [1], and of CDF (320 pb<sup>-1</sup>,  $e$  and  $\mu$  channels) [21]. The improvement in sensitivity obtained with this analysis is clearly visible in the region where we have best sensitivity for low Higgs mass discovery, i.e. 115–135 GeV.

## IX. SUMMARY

The  $\ell + \cancel{E}_T + \text{jets}$  final state has been studied on 371–385 pb<sup>-1</sup> of data taken between April 2002 and September 2004. The  $W + 2$  jet channel has been analyzed in detail. The ALPGEN event generator, which performs at leading order in QCD and EW interactions the calculation of exact matrix elements of the elementary processes involved, describes correctly, within the current statistics, the kinematic properties (jet spectra,  $W$  transverse mass) of these events.

We observe 25  $W + 2$  jet events with both jets  $b$ -tagged using the Jet Lifetime Probability (JLIP) algorithm. The production rate of these double  $b$ -tagged events is in agreement with the expectation from standard model processes, within statistical and systematic errors. For this data sample, the  $Wb\bar{b}$  expectation is  $10.8 \pm 2.4$  events compared to a total expectation of  $27.9 \pm 4.2$  events.

The number of events with a  $W$  boson candidate and two jets in which one of the jets has been  $b$ -tagged with a tighter tagging cut, and which does not belong to the double tag sample is 51 for an expectation of  $49.2 \pm 10.0$  events. The single  $b$ -tagged production rate is consistent with the simulated expectation and the kinematic distributions of these events are well described by the simulation.

To search for a Higgs boson, we have restricted the previous selections (single  $b$ -tagged and double  $b$ -tagged) to dijet mass windows of  $\pm 25$  GeV around the reconstructed Higgs masses. With these inputs, we have set using the  $CL_S$  method combined upper cross section limits between 2.4 and 2.9 pb at 95% C.L. on  $\sigma(p\bar{p} \rightarrow WH) \times B(H \rightarrow b\bar{b})$  for Higgs masses between 105 and 145 GeV.

## Acknowledgments

We thank the staffs at Fermilab and collaborating institutions, and acknowledge support from the Department of Energy and National Science Foundation (USA), Commissariat à l’Energie Atomique and CNRS/Institut National de Physique Nucléaire et de Physique des Particules (France), Ministry for Science and Technology and Ministry for Atomic Energy (Russia), CAPES, CNPq and FAPERJ (Brazil), Departments of Atomic Energy and Science and Education (India), Colciencias (Colombia), CONACyT (Mexico), Ministry of Education and KOSEF (Korea), CONICET and UBACyT (Argentina), The Foundation for Fundamental Research on Matter (The Netherlands), PPARC (United Kingdom), Ministry of Education (Czech Republic), Natural Sciences and Engineering Research Council and West-Grid Project (Canada), BMBF (Germany), A.P. Sloan Foundation, Civilian Research and Development Foundation, Research Corporation, Texas Advanced Research Program, and the Alexander von Humboldt Foundation.

- 
- [1] DØ Collaboration, *A search for  $Wb\bar{b}$  and  $W$  Higgs Production in  $p\bar{p}$  Collisions at  $\sqrt{s} = 1.96$  TeV*, *Phys. Rev. Lett.* **94**, 091802 (2005).
  - [2] DØ Collaboration, *Search for  $Wb\bar{b}$  and  $WH$  Production in  $p\bar{p}$  Collisions at  $\sqrt{s} = 1.96$* , DØ Conference-Note 4896-CONF, <http://www-d0.fnal.gov/Run2Physics/WWW/results/prelim/HIGGS/H12/H12.pdf>
  - [3] DØ Collaboration, in preparation for submission to *Nucl. Instrum. Methods Phys. Res. A*, and T. LeCompte and H.T. Diehl, *The CDF and D0 Upgrades for Run II*, *Ann. Rev. Nucl. Part. Sci.* **50**, 71 (2000).
  - [4] DØ Collaboration, *Nucl. Instrum. Methods Phys. Res. A* **338**, 185 (1994).
  - [5] Luminosity ID group: [http://www-d0.fnal.gov/phys\\_id/luminosity/data\\_access/](http://www-d0.fnal.gov/phys_id/luminosity/data_access/)
  - [6] J.-R. Vlimant et al., *Technical description of the T42 algorithm for the calorimeter noise suppression*, DØ-Note 4146.

- [7] G. Bernardi, E. Busato and J-R. Vlimant, *Improvements from the T42 Algorithm on Calorimeter Objects Reconstruction*, DØ-Note 4335.
- [8] The matrix method allows to derive the QCD background directly from data, using a “tight” and a “loose” sample, after having measured the ID probability for a loose lepton candidate to also be identified as tight, a) for leptons coming from  $W$  decays, and b) for non-isolated or fake leptons.
- [9] T. Sjostrand, P. Eden, C. Friberg, L. Lonnblad, G. Miu, S. Mrenna and E. Norrbin, *High-energy-physics event generation with PYTHIA*, Comput. Phys. Commun. **135**, (2001) 238.
- [10] H. L. Lai et al., *Improved Parton Distributions from Global Analysis of Recent Deep Inelastic Scattering and Inclusive Jet Data*, Phys.Rev. D55 (1997) 1280.
- [11] A. Pukhov et al., COMPHEP, hep-ph/9908288 (1999).
- [12] M. Mangano et al., ALPGEN, a generator for hard multiparton processes in hadron collisions, hep-ph/0206293.
- [13] J. Campbell and K. Ellis, MCFM, *Montecarlo for FeMtobarn processes*, <http://mcfm.fnal.gov/>
- [14] Y. Fisyak and J. Womersley, DØ-Note 3191.
- [15] D. Bloch et al., *Jet Lifetime b Tagging*, DØ-Note 4069.
- [16] DØ Collaboration, *b-jet identification at DØ*, in preparation.
- [17] The variable  $H_T$  is defined as the scalar sum of the transverse momentum of the jets.
- [18] DØ Collaboration, *Evidence for  $Z \rightarrow b\bar{b}$  production the DØ detector*, DØ Conference-Note xxxx-CONF, <http://www-d0.fnal.gov/Run2Physics/WWW/results/prelim/HIGGS/H12/H12.pdf>
- [19] T. Junk, Nucl. Instrum. Meth. A434, p. 435-443, 1999.
- [20] W. Fisher, DØ-Note 4975.
- [21] CDF Collaboration, *Search for  $H \rightarrow b\bar{b}$  Produced in Association with W Bosons in  $p\bar{p}$  Collisions at  $\sqrt{s} = 1.96$  TeV*, hep-ex/0512051, Accepted in Phys. Rev. Lett.

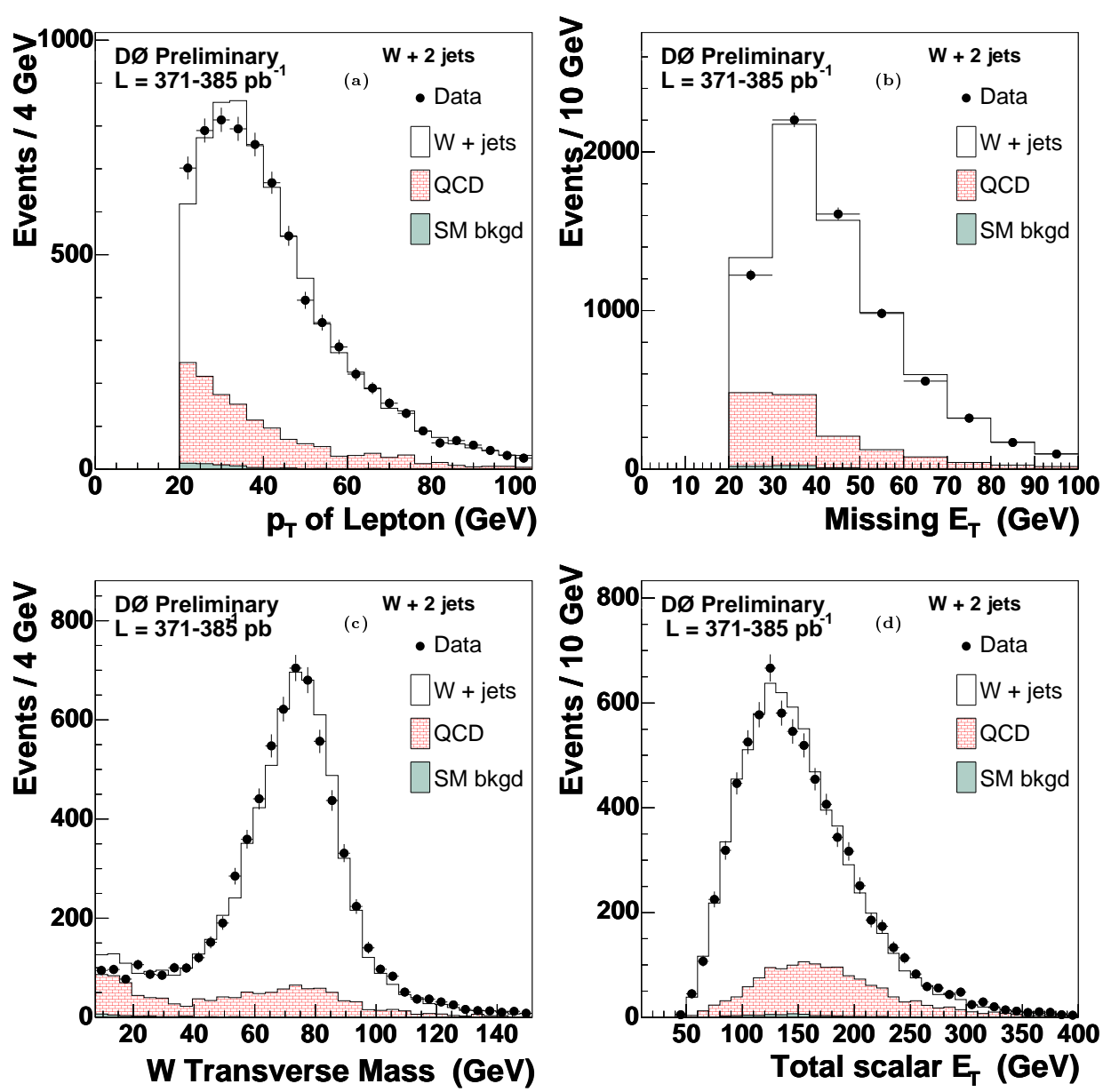


FIG. 1: Distributions of the lepton momentum (a), the missing transverse energy (b), the transverse  $W$  mass (c), and the scalar transverse energy (d) compared to the simulated expectation in the  $W + 2$  jet event sample. The simulation is normalized to the integrated luminosity of the data sample using the expected cross sections (absolute normalization) except for the  $W +$  jets sample which is normalized to the  $W + 2$  jet data, taking into account all the other backgrounds.

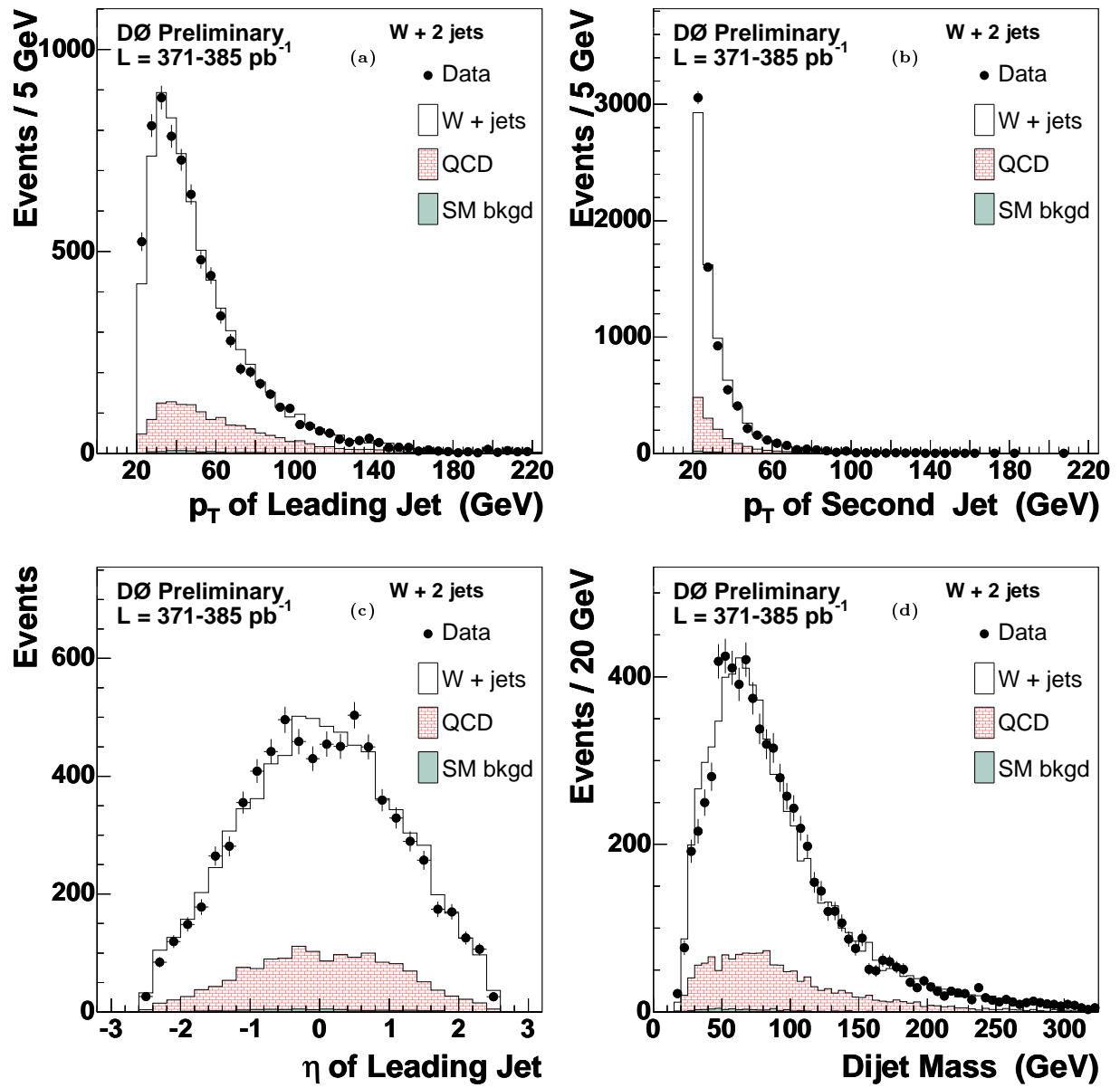


FIG. 2: Distribution of the  $p_T$  of the leading (a) and next to leading (b) jet, of the pseudorapidity of the leading jet (c), and of the dijet mass (d) between the two jets in the  $W + 2$  jet sample compared with the simulated expectation. The simulation is normalized to the integrated luminosity of the data sample using the expected cross sections (absolute normalization) except for the  $W + 2$  jets sample which is normalized to the  $W + 2$  jet data, taking into account all the other backgrounds.

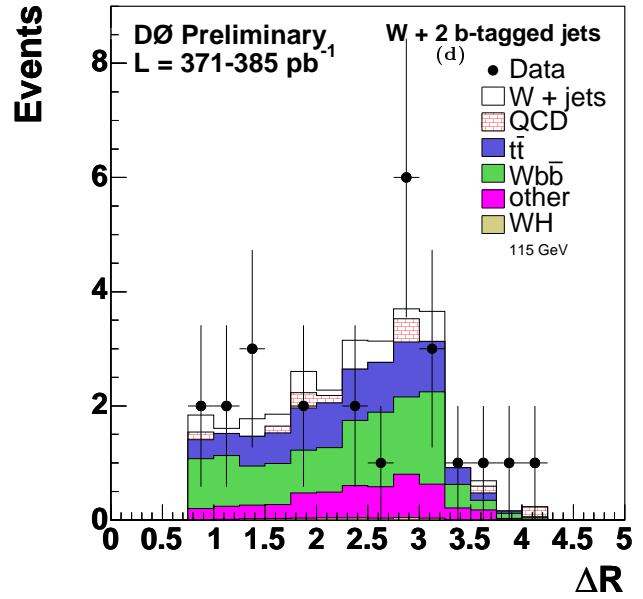
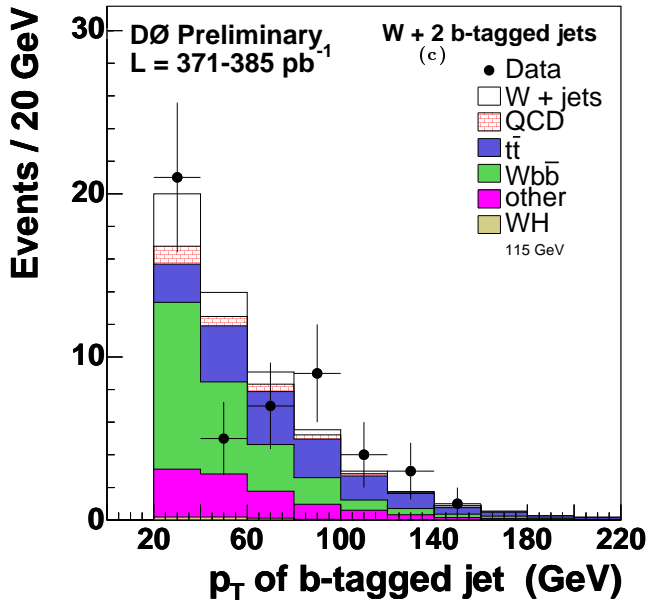
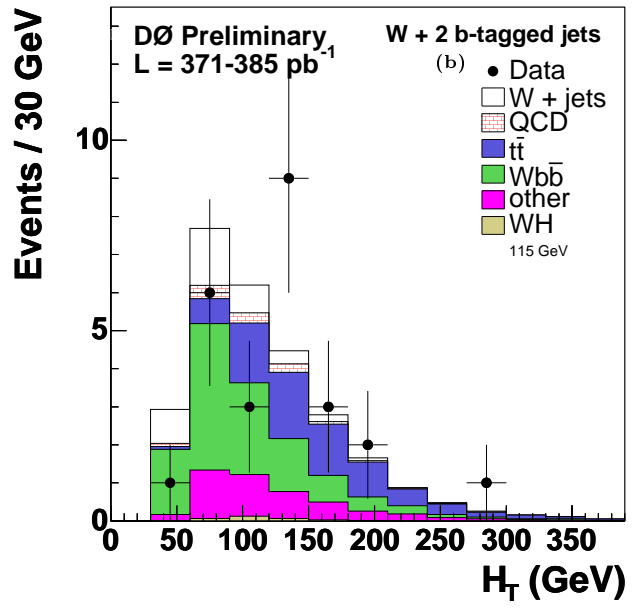
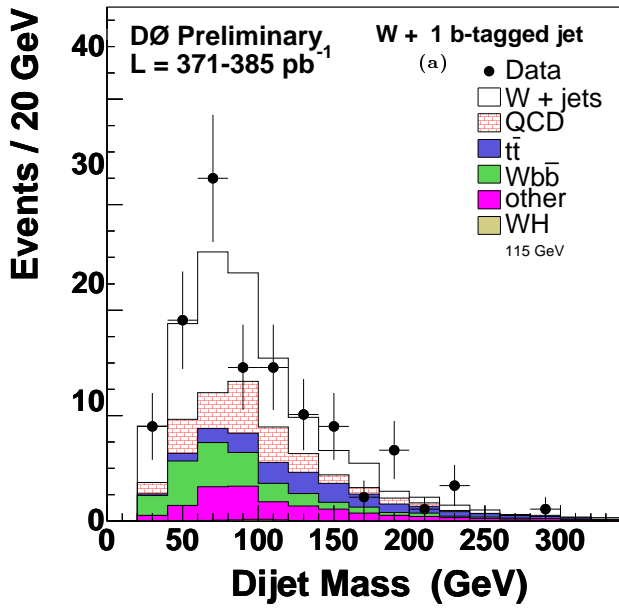


FIG. 3: a) Dijet invariant mass in  $W + 2$  jets events having one jet  $b$ -tagged; (b,c,d): Distributions for the  $W + 2$  jets events having their two jets  $b$ -tagged: b)  $H_T$  variable; c)  $b$ -tagged jets momentum; d)  $\Delta R$  between the two jets. The data are compared to the different simulated processes. The simulation is normalized to the integrated luminosity of the data sample using the expected cross sections (absolute normalization) except for the  $W +$  jets sample which is normalized to the  $W + 2$  jet data, taking into account all the other backgrounds.

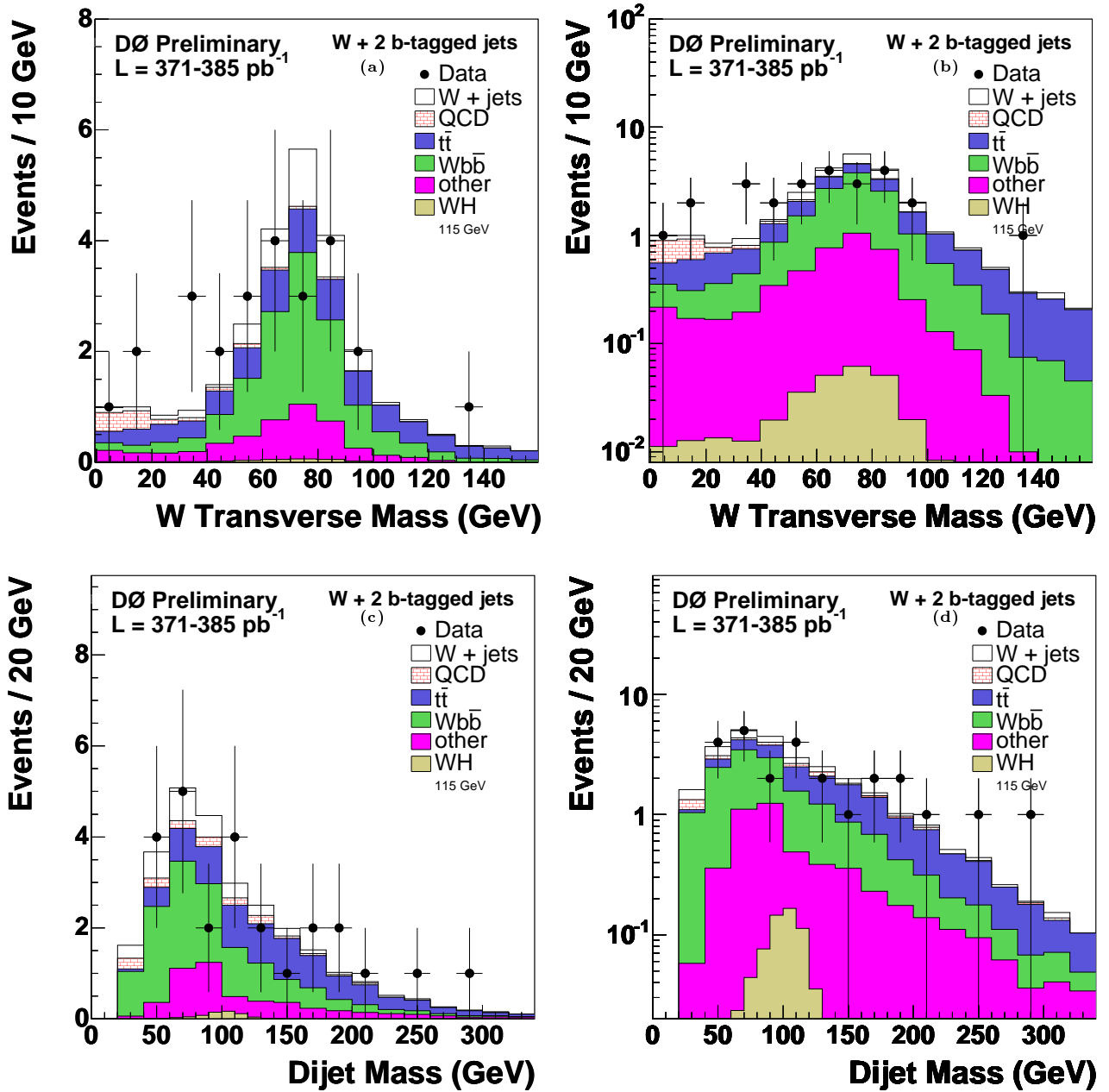


FIG. 4: Distributions for the  $W + 2$  jets events when the two jets are  $b$ -tagged. The data are compared to  $Wb\bar{b}$ ,  $t\bar{t}$ ,  $W + \text{jets}$ , and other smaller expectations. The simulated processes are normalized to the integrated luminosity of the data sample using the expected cross sections (absolute normalization) except for the  $W + \text{jets}$  sample which is normalized to the  $W + 2$  jet data, taking into account all the other backgrounds. The backgrounds labelled as “other” in the figure are dominated by single-top production. a)  $W$  transverse mass; b) same distribution in logarithmic scale; c) dijet invariant mass; d) same distribution in logarithmic scale; Also shown is the contribution expected for standard model  $WH$  production, with  $m_{\text{Higgs}} = 115 \text{ GeV}$ .

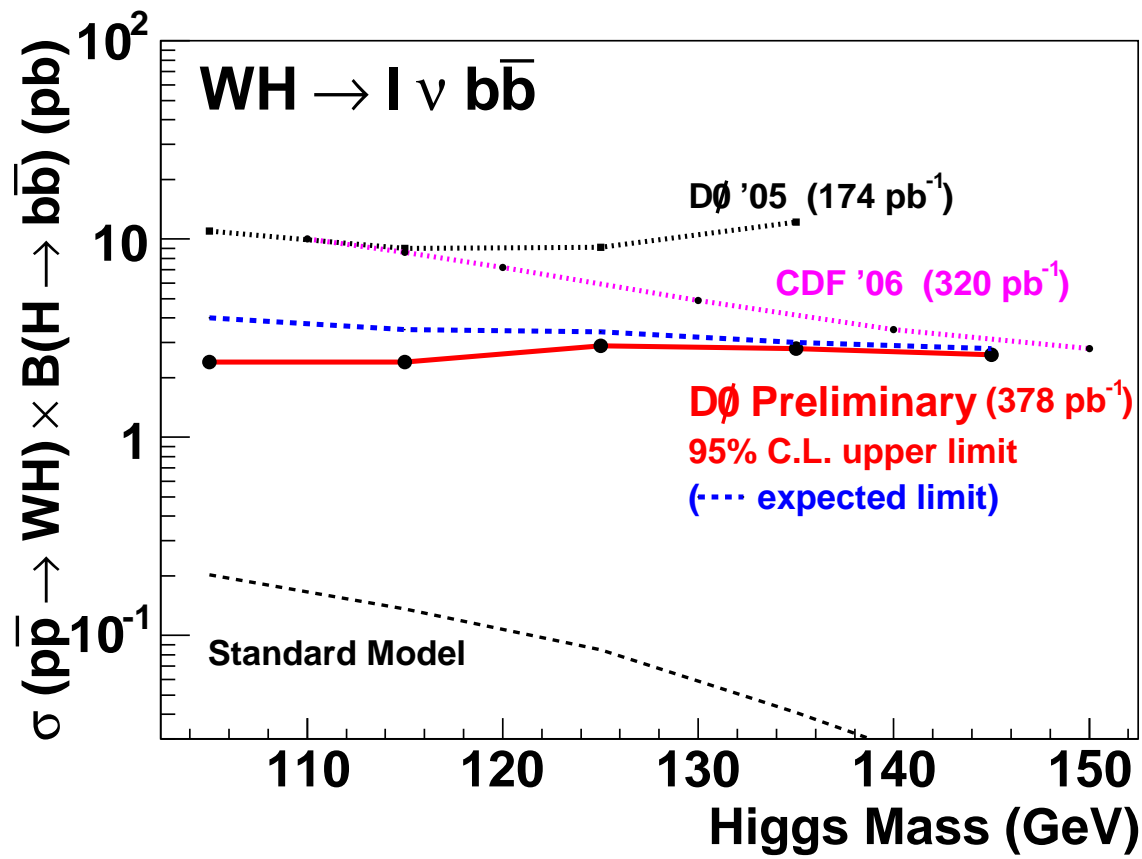


FIG. 5: 95% confidence level upper limit on cross section times branching ratio  $\text{B}(\text{H} \rightarrow \text{b}\bar{\text{b}})$ , and corresponding expected limit, obtained by this analysis with an average integrated luminosity of  $378 \text{ pb}^{-1}$ , on  $\text{WH}$  production ( $W$  boson decaying into a lepton + neutrino and Higgs into  $\text{b}\bar{\text{b}}$ ) versus Higgs mass. Also shown are the D0 analysis using the electron channel only ( $174 \text{ pb}^{-1}$ ), published in 2005, the CDF published analysis ( $e, \mu$  channels,  $320 \text{ pb}^{-1}$ , 2006) and the Standard Model expectation.